表1　バイオ医薬品の開発の広がりと医療費の高騰

売上順	一般名	薬効等	百万ドル
1	アトルバスタチン	高脂血症	13,476
2	クロピドグレル	抗血小板薬	9,291
3	サルメテロール フルチカゾン	抗喘息薬	7,737
4	リツキシマブ	非ホジキンリンパ腫	6,739
5	エタネルセプト	関節リウマチ/乾癬	6,447
6	インフリキシマブ	関節リウマチ/クローン病	6,230
7	バルサルタン	抗圧剤	6,227
8	エソメプラゾール	抗潰瘍剤	5,200
9	エポエチン　アルファ	腎性貧血	5,116
10	ベバシズマブ	抗がん剤	4,933
11	トラスツズマブ	抗がん剤	4,824
12	オランザピン	統合失調症	4,696
13	フマル酸クエチアピン	統合失調症	4,656
14	モンテルカス	抗喘息	4,582
15	アダリムマブ	関節リウマチ	4,359

世界の大型医薬品売り上げ高ランキング（2008）http://www.utobrain.co.jp/news-release/2009/0730/NewsRelease0730.pdf

- 2018年に新薬の中に占める抗体医薬品の比率は30%になる
  Reichert, M. J.; Monoclonal Antibodies as Innovative Therapeutics. Current Pharmaceutical Biotechnology, 9, 423-430（2008）
- National Institute for Health and Clinical Excellenceが，Avastin と Erbitux は高価過ぎて使用を推薦できず
  Colorectal Cancer：Bad NICE News for Avastin and Erbitux
  Posted on：Monday, 21 August 2006, 12：00 CDT
  The UK's National Institute of Clinical Excellence has decided against making Avastin and Erbitux available for the treatment of colorectal cancer on the National Health Service, arguing that both drugs are too expensive.
  UK's NICE Recommends Use Of Erbitux For Metastatic Colorectal Cancer Patients
  02 Jun 2009

ると期待されている。もうひとつは，抗体の血管内皮細胞でのリサイクリングに関与するFcRnに対する親和性を改変する技術で，よりFcRnに親和性を持たせることにより血中半減期の延長をもたらす[2)]。これらの2つの技術は開発が進むモノクローナル抗体医薬品をより低用量で使用可能にする技術であり，大量投与が必要とされてきた抗体医薬品の適用に変革をもたらす可能性がある。

このような動きは医薬品全体の中でのバイオ医薬品のプレゼンスが増大するに従い，医療費の高騰や患者の負担の増加に対する対応として出てきたといえる。このような対応を含めバイオ医薬品製造における技術革新は目覚しいものがあり，いくつかの製造技術が相互にそれぞれの欠点を補う形で開発が進められている。本稿では，バイオ医薬品の生産技術開発の世界動向について概説すると共に，それぞれの技術がどのように関連するか，またバイオ医薬品のライフサイクルを踏まえて今後についての大胆な予測も書いてみたい。また，製造技術開発における安全性や品質管理で話

題になった点についても触れてみたい。

2. *Escherichia coli* 等の原核生物を細胞基材とする医薬品生産

インスリンやヒト成長ホルモンなどの組換えDNA技術応用タンパク質医薬品（組換え医薬品）の開発から30年以上にもなる。新規に承認されるバイオ医薬品は動物細胞を用いたものが多いが，抗体医薬品でもターゲット分子との結合だけを目的とする場合にはFabを*E. coli*で製造することも行われている。効率的な生産のために，プロテアーゼの少ない宿主を用いたり，封入体などの生産部位の選択によりきわめて高い生産性が達成されている。また，ベクターと宿主の組み合わせについても非常によく研究されており，ある意味非常に成熟した技術といえる。

安全性の観点から，ウシ海綿状脳症（BSE）を受けウシペプトンを用いる方法から，植物分解物や無機塩類のみの製造も開発がおこなわれてきており，問題点はすべての培養液の組成を既知物質だけにするとコストの面で非常に高くなってしまうことであろう。また，抗体医薬品のFabのみを発現させた場合には，全抗体分子と異なり血中半減期が短いことが問題とされている。単純タンパク質の血中半減期を延長させる改変として，ポリエチレングリコール等を結合させる試みが行われている[3]。すでに，PEGインターフェロン類やPEG化抗体などいくつかの製品が市販されている[4,5]。

不純物としてエンドトキシンとECPがある。1980年代の初期のヒト成長ホルモン（hGH）の生産では宿主大腸菌タンパク質（ECP）の混入量が多いためにアジュバント効果が見られ，初期臨床試験では抗hGH抗体の産生が見られた。精製法の改良によりECPの混入量を低減化し，抗体産生は殆ど見られなくなった。hGHのバイオ後続品であるオムニトロープの初期臨床試験で抗hGH抗体の産生が見られたが，ECP量を低減化することにより抗体産生は見られなくなった[6]。このオムニトロープ開発における初期臨床試験の結果は，バイオ医薬品開発初期の経験が適切に生かされていなかったことを意味しており，*E. coli*を用いたタンパク質医薬品製造の思わぬ落とし穴であったといえる。

単純タンパク質医薬品開発では今後も*E. coli*等の原核生物を用いた製造は重要な技術として汎用されていくと思われるが，一方で，より生産性の高い細胞基材を用いた開発も進められている。ただ，*E. coli*を用いた経験は非常に重要であり，新たな細胞基材を開発していくに際してもECPの免疫反応性への関与を常に念頭におく必要がある。

3. CHO細胞等の動物細胞を用いたタンパク質医薬品の生産

単純タンパク質から糖タンパク質の生産の歴史を振り返ってみると，開発ストラテジーの変遷と，一度技術が出来上がってしまうと他の技術の導入が余り進まないという保守的な側面が見えてくる。組織プラズミノーゲン活性化因子（tPA）やエリスロポエチンなどの糖タンパク質の生産には動物細胞が必要とされ，複数の株化細胞が用いられていた。また，ヒトリンパ球細胞であるNAMALWA細胞やBALL細胞を生産基材として製造されるインターフェロンαなど様々な細胞が用いられていたが，生産効率の高さなどからCHO細胞が汎用されるようになった[7,8]。CHO細胞が生産基材として用いられ始めた初期には牛胎児血清が用いられていたが，培養後のバルクハーベストにおける目的タンパク質の純度やBSE発症によりリスク回避を目的として無血清化技術が飛躍的に進んだ。さらに，大量培養を行うために浮遊培養の開発が行われ，5,000L培養槽を用いた生産が一般的に行われている。

無血清培養が可能になったことにより，バルクハーベストの目的タンパク質の純度は飛躍的に向上しており，場合によっては目的タンパク質が70%を超えることもあるようで，高い純度はその後の精製工程の負荷の軽減に大きく寄与している。

一方で無血清培地の改良も大きく進み，モノクローナル抗体医薬品の製造では培養液1L当たり数gから10gの生産が可能とまで言われている。このように極めて高い生産性が達成されているが，CHO細胞を用いる生産技術としてほぼ成熟されている感がある。CHO細胞を用いるタンパク質生産は，目的タンパク質をコードする遺伝子導入と導入された細胞内でのメトトレキセートによるコピー数の増幅によって高い生産性がもたらされている。

CHO細胞以外の動物細胞でのタンパク質生産では，より生産性の高い細胞の選択[9]や，目的タンパク質遺伝子のコピー数を増加させるために工夫[10]が行われている。開発中のこれらの技術については本稿では触れられなかったが，将来この技術が実用化されてくる可能性も十分あり得る。一方で，CHO細胞での経験は，単にタンパク質の生産ばかりでなく内在性のウイルス様粒子の解析，宿主タンパク質の管理など多くの製造のノウハウが蓄積されており，新たな生産手段の導入に際してはこのようなCHO細胞を用いた生産の経験をどのように生かすか，あるいは独自の経験をどのようにして蓄積していくかが大きな鍵を握ると考えられる。

モノクローナル抗体の生産では，CHO細胞以外にNS0細胞やSP2/0細胞のようにマウスミエローマ細胞が汎用されている。これは，ミエローマ細胞を用いることにより重鎖（H鎖）および軽鎖（L鎖）それぞれ2分子ずつから構成される抗体分子の発現に有用であるとの技術的要因にあると思われる。一方で，NS0細胞やSP2/0細胞ではマウス型の糖鎖が付加され，ヒトが持つ異種糖鎖抗原付加によるアナフィラキシーの発症のリスクもあり得る[10]。但し，糖鎖の付加部位によっては異種抗原糖鎖が付加しても必ずしも反応性があるわけではなく，抗体のFc領域のコンセンサス糖鎖ではGalα1-3Galといった異種抗原糖鎖が結合しても必ずしもアナフィラキシー発症リスクがあるわけではないとされている。

一方で，動物細胞を用いた培養工程では培養スケールの大きさが非常に重要となる。特に浮遊細胞系では酸素の安定供給と老廃物の除去のために攪拌操作が非常に重要であるが，大量培養になれば十分に攪拌するために回転翼の回転速度を増加させる必要があり，その回転翼による細胞のせん断が細胞の生存率に影響を与える可能性が高くなる。また目的タンパク質の翻訳後修飾にも大きな影響を与える。FDAは，培養細胞を用いたバイオ医薬品の製造において5,000Lから25,000Lといった培養スケールの大幅な変更申請に対して製法変更とは認められないという結論を出したケースもあった。このように製造スケールの変更における製造変更の同等性評価は今後の大きな課題となっている。

動物培養細胞を用いたバイオ医薬品の製造で，どのような細胞を選択するかは目的タンパク質の特性や生産効率，翻訳後修飾などを考慮して選択していく必要がある。一方で，CHO細胞やNS0細胞，SP2/0細胞といった製造経験の多い細胞は，製造におけるタンパク質修飾や生産性についてのデータが豊富に蓄積されており，さらにウイルス安全性面からも蓄積された情報を活用しやすいという利点がある。このために新たな細胞基材を用いるのはハードルが高いとされている。

その一方で，糖タンパク質はこれまでCHO細胞等の動物タンパク質を用いてしか製造されないとされてきたが，酵母を用いた糖タンパク質製造の試みがなされている[11,12]。もし酵母を用いた糖タンパク質の製造が実用化レベルにいたれば，これまで動物細胞を用いた開発で，必須とされてきたウイルス安全性の評価に要していた解析時間やリソースを省くことが可能になり，製法開発のスピードが上がる可能性がある。タンパク質の特性を考慮しつつ生産系をどのように選択していくかは今後の大きな課題と思われる。

4. トランスジェニック動植物を用いたバイオ医薬品の製造

バイオ医薬品を製造するのに，動物や植物に目的タンパク質遺伝子を導入してトランスジェニッ

ク（Tg）動物や植物を作製する技術が注目を集めている。既にTg動物製品は2品目が海外で市販されており，実用化の時代に入っている。Tg動物を用いたバイオ医薬品に関してはEUでは1994年にガイドライン[13]が発出されており，FDAはバイオ医薬品に関するガイドラインではないがTg動物作製に当たってのガイダンス案を出している[14]。我が国ではTg動物に関する指針や通知は発出されていないために，規制上の要件に関しては，これらの欧米ガイドラインが参考になる。

ここでは，Tg動物を用いる場合の安全性や品質のキーポイントになる点について言及する。

Tg動物を用いる生産では，無菌動物やウイルスフリー動物を用いることは余り現実的ではないことから，ウイルス安全性に対する対応が重要となる。特に内在性のレトロウイルスや潜在しているウイルスに関する試験や，原料にウイルスが混入していることを前提としての精製工程でのウイルスクリアランス試験とその評価が重要である。従って，①生産用Tg動物作製に用いる動物種の選択とウイルス等の試験，②製造過程がどの程度ウイルス除去および不活化能力を有するかに関する評価，③原料バルクなど製造工程の適当な段階における製品のウイルス否定試験などの3つのアプローチを採用し，相互補完的にウイルス安全性を確保する必要がある。また平行して，動物の飼育工程での迷入ウイルスに対する試験も重要であり，そのためには飼育環境，飼料等からの汚染の可能性をできる限り低減することも重要である。

一方で，動物由来タンパク質や多糖類を医薬品として利用しており，これらのウイルス安全性確保では生物由来原料基準の中の動物由来原料基準を適用するべきと考えられる[15]。また，局方参考情報「日局生物薬品のウイルス安全性確保の基本要件」も参考にするべきであろう。ここでは，食肉基準への適合と健康な動物の要件が記載されており，Tg動物由来バイオ医薬品の製造にも適用できる要件もあると考えられる。

Tg植物製品についてはEUおよびFDAからガイドライン（FDAは案）が発出されており，Tg植物を用いたバイオ医薬品の製造における品質や安全性評価のポイントが示されている。特に，Tg植物で製造されたタンパク質の翻訳後修飾が動物細胞を用いた場合と大きく異なる可能性があり，植物特有の糖鎖修飾はヒトに対して異種抗原となる可能性があり，そのために糖転移酵素の導入やノックダウンを行う遺伝子改変されたTg植物に目的遺伝子を導入することが行われている。ただ，これらの糖鎖修飾酵素をヒト型に改変できているわけではなく，また改変によっては植物の成長そのものに影響を与える可能性があり，現実的には目的タンパク質の特性に応じた宿主植物の改変によって製造法を確立していく必要がある。糖鎖以外にも植物特有のリン酸化や脂質付加などが起こる場合もあり，これらの修飾がどの程度ヒトでの安全性に関与するかが明らかになっていないことも多い。

Tg植物由来タンパク質医薬品が先進国で承認された製品は無いが，Tg動物由来製品以上にコストの低減化が期待されている。例えば，EUではTg植物由来製品に関するコンソーシアム[16]が作られており，この中にはムコ多糖症治療薬のような希少疾病薬製品をTg植物を用いて製造することにより医療費の低減化を図りたいとの狙いがある。ムコ多糖症治療用タンパク質医薬品では，年間での投与に要する費用が数千万円にも上る場合があり，大量投与されるバイオ医薬品を植物を用いて製造することが可能になれば，患者の負担軽減や医療費の軽減に寄与できると考えられる。

また，Tg植物由来製品の中には果実や野菜のように食品の形態で摂取するものの中に目的タンパク質を発現させ，そのタンパク質に対する抗体産生を目的とする“食べるワクチン”開発も進められている。食べるワクチンは有効成分の含量をどのように管理するのか等いくつかの課題があるが，注射製剤と異なり感染性因子に対する管理が比較的容易であり，精製工程が簡便であり無菌製造工程を行わないですむことから製造コストが極めて低く抑えられるという利点がある。

5. 核酸医薬品やペプチド合成技術

これまで述べてきたバイオ医薬品の製造は細胞や動物，あるいは植物といった生物を生産手段として用いるものである。生物を生産手段として用いることにより，転写，翻訳，翻訳後修飾といった生物の持つ巧妙なタンパク質産生機構を利用することでより複雑なタンパク質合成を可能としている。その一方で，生きている生物を利用することによる生産の揺らぎがあり，品質の恒常性を担保するためには製造条件の厳密な管理が必要とされる。また，生産基材によってはウイルス等の感染性因子に対する安全性確保が重要な課題となっている。

一方で，化学合成されたペプチドや低分子の核酸の医薬品としての利用が既に行われている。例えばペプチドの合成技術は非常に向上してきており，またそのコストも非常に低減化されている。合成が可能なペプチドの大きさも改良が重ねられており，従来は組換えDNA技術を用いて製造されていたペプチドも合成法によって製造可能になりつつある。

もう一方で，抗体などの複雑な分子の機能を28アミノ酸で代用できることが示され[17]，ペプチド医薬品が抗体医薬品の代用として使われる可能性も視野に入れられている。また，サイトカインや増殖因子の機能を真似る（ミミック）医薬品としてペプチドミミックの開発も精力的に進められている。このような新たな開発戦略により，ペプチド合成技術が注目されている。

核酸医薬としては特定の遺伝子発現をノックダウンさせるアンチセンスオリゴヌクレオチドやRNA緩衝因子であるsiRNA，さらには特定の遺伝子の転写因子と結合するデコイ核酸など，タンパク質の翻訳や機能発現を細胞内で制御するためのオリゴヌクレオチド技術の開発が進められている。それ以外のオリゴヌクレオチド技術として特定のタンパク質との結合性を有するアプタマーの開発が注目されている。細胞内で作用するアンチセンスオリゴヌクレオチドやsiRNA等は特定の細胞への送達と細胞内へ取り込ませるDDS技術の開発が必須であり，このDDS開発が大きな課題となっている。アプタマーは抗体のような利用法が可能であり，すでに加齢性黄斑症の治療薬として市販されている。

上記したペプチドや核酸医薬は将来バイオ医薬品の代替として用いられるようになる可能性が考えられる。また，前項で述べたTg植物やTg動物を用いたバイオ医薬品の製造もCHO細胞等での製造に変わって用いられてくるようになる可能性がある。すなわち，バイオ医薬品の製造技術の変化は，近い将来におけるバイオ医薬品のライフサイクルを考える上でも重要である。このような考え方を**図1**にまとめてみた。今回は取り上げられなかったが，細胞治療や遺伝子治療といった製品もバイオ医薬品製造におけるライフサイクルと切り離しては考えられなくなると予想している。

6. おわりに

バイオ医薬品の生産に，多様な製造技術が開発されるようになってきており，今回は触れることができなかったが，我が国が得意とするカイコを用いた医薬品の製造やニワトリといったこれまでにない技術開発も行われてきている。

バイオ医薬品の製造手段としてどれを選択していくかは目的タンパク質の特性に応じて柔軟に考えるべきと思われるが，一方で従来の手法から新しい製造技術を導入するには経験の蓄積が生かせないという側面もある。従って全く異なる生産基材，例えばTg植物を用いてバイオ医薬品を製造する場合に，もし同種製品が既にCHO細胞等を用いて製造されている場合には既存の製品との比較が極めて有用な情報をもたらしてくれる可能性がある。新たな生産手法を導入するメリットは，おそらくコストの削減であったり，感染因子のリスクの低い生産基材の選択であることが想定され，そのメリットと新規生産技術採用に際して払うべきリソースの大きさが重要であろう。一方で，バイオ医薬品開発は，今後も益々拡大していくことが予測され，医療費の増大や患者負担を考

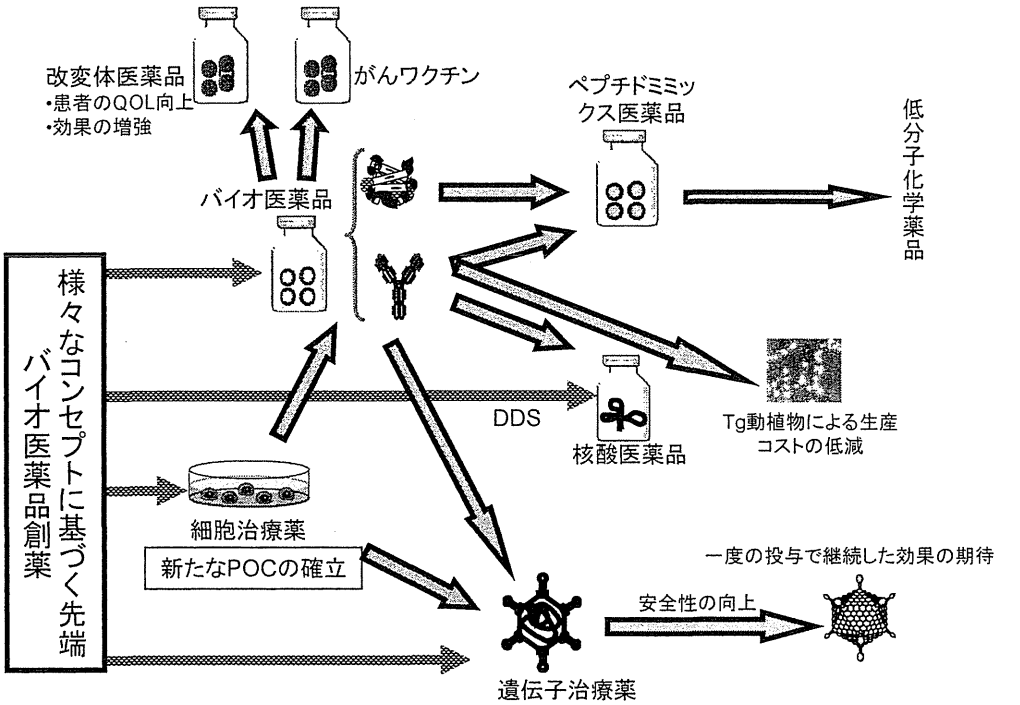

図1　今後のバイオ医薬品の製造戦略

従来の *E. coli* やCHO細胞等を用いたバイオ医薬品の生産から，より生産効率の高い細胞やTg動植物を用いた生産の取り組みが続けられると予想される。また，タンパク質の代わりに，同様の生物活性を持つ低分子ペプチドや核酸医薬の開発も現実性が出てきている。また，有用タンパク質を産生する細胞を直接ヒトに投与したり，遺伝子治療薬としての利用も近いと考えられる。

えると，より効率的かつ安全性の高い製造技術の開発が望まれている。

文　　献

1) S. Iida *et al.*, *Clin. Cancer Res.*, **12**, 2879-2887 (2006)
2) T. Igawa *et al.*, *Nature Biotech.*, **28**, 1203-1208 (2010)
3) M. J. Roberts *et al.*, *Advanced Drug Delivery Reviews*, **54**, 459-476 (2002)
4) R. B. Pepinsky *et al.*, *J. Pharmacol. Exp. Therapeu.*, **297**, 1059-1066 (2001)
5) A. Kozlowski *et al.*, *J. Controlled Release*, **72**, 217-224 (2001)
6) Omnitrope EMA Scientific Discussion：http://www.ema.europa.eu/docs/en_GB/document_library/EPAR_-_Scientific_Discussion/human/000607/WC500043692.pdf
7) J. Chusainow *et al.*, *Biotech. Bioengineer.*, **102**, 1182-1196 (2009)
8) T. Yoshikawa *et al.*, *Cytotechnology*, **33**, 37-46 (2000)
9) F. M. Wurm *et al.*, *Nature Biotech.*, **22**, 1393-1398 (2004)
10) M. W. Saif *et al.*, *Cancer Chemother Pharmacol.*, **63**, 1017-1022 (2009)
11) S. R. Hamilton *et al.*, *Current Opinion Biotech.*, **18**, 387-392 (2007)
12) P. P. Jacobs *et al.*, *Current Molecul. Medicine*, **9** (7), 774-800 (2009)
13) Use of transgenic animals in the manufacture of biological medicinal products for human use legislative basis Directive 75/318/EEC as amended date of first adoption. December 1994 none/III/3612/93
14) Guidance for Industry：Regulation of Genetically Engineered Animals Containing Heritable Recombinant DNA Constructs. FDA 2009 (http://www.fda.gov/AnimalVeterinary/

GuidanceComplianceEnforcement/GuidanceforIndustry/default.htm)
15) 生物由来原料基準. 2003年5月20日制定（平成15年厚生労働省告示第210号）
16) J. K-C. Ma *et al.*, *EMBO Rep.*, **6**, 593-599 (2005)
17) R. C. Ladner, *Nature Biotech.*, **25**, 875-876 (2007)

◇ ◇ ◇ ◇

Journal of Bioscience and Bioengineering
VOL. 115 No. 1, 104–110, 2013

ELSEVIER

www.elsevier.com/locate/jbiosc

Aggregation analysis of pharmaceutical human immunoglobulin preparations using size-exclusion chromatography and analytical ultracentrifugation sedimentation velocity

Elena Krayukhina,[1] Susumu Uchiyama,[1] Kiyoko Nojima,[2] Yoshiaki Okada,[2] Isao Hamaguchi,[2] and Kiichi Fukui[1,*]

Graduate School of Engineering, Osaka University, 2-1 Yamadaoka, Suita 565-0871, Japan[1] and Department of Safety Research on Blood and Biological Products, National Institute of Infectious Diseases, 4-7-1 Gakuen Musashi-Murayama-shi, Tokyo 208-0011, Japan[2]

Received 27 June 2012; accepted 31 July 2012
Available online 24 August 2012

In the pharmaceutical industry, analysis of soluble aggregates in pharmaceutical formulations is most commonly performed using size-exclusion chromatography (SEC). However, owing to concerns that aggregates can be overlooked by SEC analysis, it has been suggested that its results should be confirmed with orthogonal methods. One of the main alternative methods for SEC is analytical ultracentrifugation sedimentation velocity (AUC-SV), which has been indicated as an important tool for the measurement of protein aggregation. The present study aimed to show that AUC-SV can be effectively applied for the characterization of marketed immunoglobulin pharmaceutical preparations to support the results obtained by SEC. In addition, the present research aimed to assess the appropriateness of two integration approaches for the quantitative analysis of the SEC results. Thus, the aggregates were measured in seven different preparations of human immunoglobulins by AUC-SV and SEC, and the acquired chromatographic data were processed by using either the vertical drop method or the Gaussian skim approach, implemented in the Empower II chromatography data software (Waters, Tokyo, Japan). The results of aggregation measurements performed using AUC-SV were in good agreement with those obtained using SEC. As expected, the Gaussian skim integration approach inherently provided lower estimates of aggregation content than the results of the vertical drop method. The finding of this study confirmed the complementary nature of AUC-SV to SEC for aggregate composition analysis and underscored the important role that the different integration methods can play in the quantitative interpretation of chromatographic results.

[**Key words:** Immunoglobulin; Size-exclusion chromatography; Vertical drop method; Gaussian skim; Analytical ultracentrifugation sedimentation velocity]

Antibody aggregation is a common problem in the pharmaceutical industry, encountered during the manufacturing process and long-term storage of antibody products. It was suggested that the presence of antibody aggregates in a therapeutic product can affect drug efficacy or may even cause immunogenic reactions when administered to patients (1). To ensure that the biotherapeutic product is consistent with quality standards and meets all regulatory requirements, an accurate measurement of aggregation content is necessary.

Size-exclusion chromatography (SEC) is currently employed for the quantification of soluble antibody aggregates as a quality control method. SEC separates molecules based on their hydrodynamic volume, provides highly reproducible results, is easy to perform, and is a relatively fast technique for the characterization of pharmaceutical formulations. The elution profiles generated by SEC are analyzed, and the fractional amount of each solute detected in the sample is estimated from the area under the peak, which is calculated using chromatographic software. In general, the area under unresolved peaks is determined by the vertical drop method. This method involves the addition of a vertical line from the valley between the peaks to the horizontal baseline. However, the perpendicular separation of overlapping peaks has previously been shown to introduce significant errors in peak area estimation (2–4). Alternative approaches implemented in chromatographic data analysis packages allow more sophisticated approaches for the identification of unresolved peaks, such as the Gaussian skim method implemented in the Empower II software. This algorithm fits the shapes of the peaks observed in the chromatogram using a Gaussian profile and is assumed to better represent the shape of the parent peak in the overlapping peaks group. Nevertheless, the vertical drop method remains the most commonly applied approach for the integration of chromatographic peaks (5). Another problem with SEC is related to a nonspecific binding of protein aggregates to the column matrix, as recently discussed (6).

The above-mentioned issues potentially affect the accuracy of SEC measurements. Thus, it has been suggested that the results of

* Corresponding author. Tel.: +81 6 6879 7440; fax: +81 6 6879 7442.
E-mail address: kfukui@bio.eng.osaka-u.ac.jp (K. Fukui).

1389-1723/$ – see front matter
http://dx.doi.org/10.1016/j.jbiosc.2012.07.021

the SEC method should be verified using different analytical techniques (7). Among alternatives to SEC method, analytical ultracentrifugation sedimentation velocity (AUC-SV) was found to be very suitable for this purpose (8).

The improvements in AUC instrumentation and data analysis packages have promoted an increase in the number of potential applications of AUC-SV (9–12). Particularly, it has been indicated as a valuable tool for monitoring antibody aggregation (8,13–16). Nevertheless, owing to the lower degree of reproducibility of AUC-SV results compared with SEC results, the implementation of AUC-SV to a routine characterization of pharmaceutical antibodies has not been successful until now. In the recent study presenting the summary opinion of the members of the protein characterization subcommittee of the European Immunogenicity Platform, it has been suggested that throughout the pharmaceutical development process, AUC should not be used for validation of SEC results but rather should be used as a complementary method for SEC (17).

The purpose of this study was to demonstrate that AUC-SV can very effectively be used for the characterization of marketed immunoglobulin preparations and to confirm the performance of SEC. Over the years, a number of studies have been performed using AUC-SV and SEC, as applied to custom monoclonal antibody formulations (13,14). In contrast, the present research was conducted using a wide range of available marketed products, consisting of four liquid formulations and three lyophilized formulations of pharmaceutical human immunoglobulin preparations. Based on the previous studies (18–20) and our own results (21), experimental and data analysis procedures for precise aggregation content measurement in immunoglobulin formulations using AUC-SV were developed. Following the established protocol, we confirmed that AUC-SV can very effectively be used to characterize marketed pharmaceutical products. To address the uncertainty that can result from application of different methods for chromatographic peak identification, we applied the vertical drop method and the Gaussian skim approach, implemented in the Empower II software to analyze SEC data. Although integration of chromatographic peaks using the vertical drop method consistently indicated a slightly greater amount of aggregates compared with the value estimated by using the Gaussian skim algorithm, we achieved good overall agreement between AUC-SV and SEC results.

MATERIALS AND METHODS

Human immunoglobulin preparations In the present study, four liquid and three lyophilized preparations of human immunoglobulins were used. Polyglobin-N 5% for intravenous injection (0.5 g/10 ml), a pH 4-treated acidic human normal immunoglobulin, was purchased from the Japanese Red Cross Society (Tokyo, Japan). Venoglobulin IH 5% for intravenous injection (0.5 g/10 ml), a polyethylene glycol-treated human normal immunoglobulin; Hebsbulin IH for intravenous injection (1000 units), a polyethylene glycol-treated human anti-HBs immunoglobulin; and Tetanobulin IH for intravenous injection (250 units), a polyethylene glycol-treated human tetanus immunoglobulin, were purchased from Benesis Corporation (Osaka, Japan). Glovenin-I for intravenous injection (500 mg), a freeze-dried polyethylene glycol-treated human normal immunoglobulin G, was purchased from Nihon Pharmaceutical Co., Ltd. (Tokyo, Japan). Gammagard for intravenous injection (2.5 g), a freeze-dried ion-exchange resin-treated human normal immunoglobulin, was purchased from Baxter Limited (Tokyo, Japan). Sanglopor for intravenous infusion (2.5 g), a freeze-dried pH 4-treated human immunoglobulin, was purchased from CSL Behring (Tokyo, Japan). For all lyophilized products, the immunoglobulin concentration in the reconstituted formulation was 50 mg/ml.

Size-exclusion chromatography SEC analysis was performed in triplicate using a high-performance liquid chromatography (HPLC) workstation (Alliance 1100 HPLC system) with a TSK gel G3000SW_{XL} column (Tosoh Bioscience, Tokyo, Japan) under standard conditions. The separation was conducted at a flow rate of 0.5 ml/min at room temperature and was monitored by UV detection at 280 nm. The elution buffer consisted of 1 mM potassium phosphate, 3 mM sodium phosphate, and 155 mM sodium chloride at pH 7.4. A minimum reproducible volume of 5 µl of antibodies at formulation concentrations was injected into the HPLC system for analysis. This prevented excessive antibody dilution, as SEC itself is known to produce a high dilution of the sample that will tend to dissociate the reversible aggregates (22). An antibody mass recovery of 94% and higher was confirmed for all studied samples and was in agreement with the values from previous studies (14,23). Chromatographic data were processed by the Empower II chromatography data software (Waters, Tokyo, Japan) using the ApexTrack integration algorithm combined with either the vertical drop method or the Gaussian skim method. The integration parameters were set at default, and Detect Shoulders event was enabled. To estimate the fractional amount of each peak, the calculated peak area was divided by the total area that was obtained by summation of the areas of the peaks, including the solvent peak, where it was present.

Analytical ultracentrifugation sedimentation velocity AUC-SV analysis was performed according to the experimental routine especially designed for the present study. It addresses specific requirements to conduct the measurement of aggregation content in immunoglobulin preparations in a very precise manner. Thus, the sedimentation experiments were conducted in a ProteomeLab XL-I analytical ultracentrifuge (Beckman Coulter) equipped with a 4-hole An60 Ti rotor. Beckman Coulter 12-mm double-sector charcoal-filled epon centerpieces manufactured after July 2008, when an improved manufacturing process was implemented by Beckman Coulter (19), and quartz windows were used for the experiments. The cells filled with 430 µl of the prepared samples were placed in the rotor and thoroughly equilibrated at 20°C and 0 rpm for approximately 1 h before beginning data acquisition. Data were recorded at 40,000 rpm and 20°C using absorbance optics at 280 nm. The scanning was performed as quickly as possible between radial positions 5.9 and 7.2 cm, with a step size of 30 µm until the sample was completely sedimented.

AUC-SV analysis of the selected preparations was complicated by the nonideality of the formulations, containing high concentrations of excipients such as sugars and sugar alcohols. Therefore, the antibody formulations were diluted to the concentration of approximately 0.5 mg/ml using buffer consisting of 1 mM potassium phosphate, 3 mM sodium phosphate, and 155 mM sodium chloride at pH 7.4. The antibody samples were prepared immediately before the AUC-SV measurement. In this way, any potential decrease in the amount of aggregates due to reversible dissociation was minimized. AUC-SV runs were performed in triplicate, with three data sets collected in each run. The same combination of rotor hole position, cell housing, windows, and centerpiece was used for all consecutive runs, as recommended previously (19). This practice helped us to identify the micro-deformation of the centerpiece systematically affecting the quality of the data acquired for the cell placed in rotor hole 3. Therefore, these data were excluded from further analysis.

The SEC analysis of the reconstituted lyophilized preparations of immunoglobulins indicated relatively slow time-dependent change in the distribution of monomeric/dimeric forms of antibody, which was negligible compared with the time of the first sedimentation experiment, performed immediately after reconstitution. However, as the time interval between the reconstitution and the beginning of the second and third experiments was longer, the distribution was significantly affected. Thus, the results of the AUC-SV analysis are presented as the mean values of six measurements performed in three independent runs for the liquid formulations and as the mean values of two measurements performed in one run for the freeze-dried formulations.

The data were analyzed using the C(*s*) method of SEDFIT ((24); http://www.analyticalultracentrifugation.com). For the analysis, the meniscus was set to the midpoint position of the absorbance spike corresponding to the air-sample boundary and was floated during the fit. It was confirmed that the fitted meniscus position was physically relevant and was still located in the vicinity of the maximum of absorbance spike. The sedimentation coefficient (*s*) range was chosen so that no partial peaks were presented at the edges of the *s*-range and was 1–15 S, 1–20 S, 1–25 S, or 1–30 S, respectively. A grid resolution was selected in a way that resolution of *s* values corresponded to 0.05 S. The frictional ratio was initialized at 1.4 and floated during the fitting procedure. A regularization level of 0.68 was used. The buffer density and viscosity were calculated using the SEDNTERP software and were 1.00516 g/ml and 1.0175 cP, respectively. The partial specific volume was kept at the SEDFIT default value of 0.73 cm^3/g, which in general provides a good estimate of the partial specific volume of proteins. The actual values could not be estimated owing to the polyclonal nature of the studied antibody formulations. The goodness of the obtained fits was evaluated by comparing the rmsd values of the resulting fits with the values obtained for the empty cells before the experiments. In this way, it was verified that all the fits had only a randomly distributed noise and that no systematic errors were introduced during the fitting routine. In addition, it was confirmed that no visible diagonal lines were present on the residuals bitmap. To estimate the relative abundance of the different species present in the samples, integration of the C(*s*) distributions was performed. The percentages of antibody monomers, oligomers, fragments, and albumin were calculated by dividing the corresponding peak area by the sum of the areas under all peaks.

RESULTS

Experimental routine for AUC-SV analysis of immunoglobulin preparations The development of an experimental routine for AUC-SV analysis of immunoglobulin preparations

followed two main phases: a systematic review of the available literature on the subject and testing of a theoretically designed protocol. First, based on the previous studies (18–20), a set of experimental parameters regarding rotor and cell components, sample concentration used for the analysis, optics applied for the detection, and software package for the data analysis were chosen. At the next step, the optimum rotational speed from the recommended range of 40,000–60,000 rpm was selected for AUC-SV analysis. Our previous study has shown that the hydrodynamic parameters of antibodies are affected by high rotational speed during sedimentation experiments, whereas the amount of dimeric antibody aggregate remained unaffected by the rotational speed (21). Thus, we excluded rotational speeds faster than 50,000 rpm from consideration, assuming that these high speeds can contribute to the imprecision of aggregation analysis. High-quality centerpieces, which have previously been shown to improve the precision of aggregates measurements, were Beckman Coulter charcoal-filled epon centerpieces. The Beckman Coulter Buyer's Guide recommends using the epon charcoal-filled centerpieces at speeds slower than 42,000 rpm. Finally, the possible presence of fast-sedimenting high-molecular weight aggregates was considered; thus a rotational speed of 40,000 rpm was selected for the AUC-SV experimental setup.

Aggregation analysis of liquid human immunoglobulin preparations The SEC chromatogram of Polyglobin (Fig. 1A) showed a major peak corresponding to the monomeric form of the antibody. The asymmetry of the monomer peak was attributed to the nonspecific binding of the highly concentrated antibody to the SEC column packing material (6), which is a common problem in protein chromatography. A shoulder peak eluted before the major peak suggested the presence of a dimeric component in the solution. When either integration algorithm was applied for the data analysis, the area under the dimeric peak was estimated to be approximately 0.8% of the total signal (Table 1). This estimate was lower compared with that obtained by AUC-SV analysis. In C(*s*) distribution (Fig. 1B), in addition to monomeric and dimeric peaks, minor peaks corresponding to antibody fragments and trimeric aggregates were observed. Nevertheless, the results of triplicate measurements showed that these species were present at amounts below the commonly accepted limit of AUC-SV quantification of 1% (25) and therefore could not be considered to be reliably measured. In addition, the standard deviation of the obtained values indicated low reliability of these estimates.

The fraction of dimeric aggregates present in the Venoglobulin formulation was higher than that estimated for Polyglobin (Table 1). Similar to Polyglobin, the AUC-SV analysis of Venoglobulin indicated the presence of trace amounts of fragments and trimeric aggregates below the accepted limit of quantification. The estimates of the total quantity of aggregates derived from AUC-SV measurements and integration of chromatogram using the Gaussian skim approach were in good agreement. The results of peak separation using the vertical drop method and the Gaussian skim approach were consistent, although the amount of dimeric aggregates calculated by the vertical drop method was slightly higher than that obtained by the Gaussian skim approach.

The results of AUC-SV and SEC obtained for Hebsbulin were in good agreement, indicating the presence of only monomeric and dimeric forms of the antibody (Fig. 1E and F). The amount of dimeric aggregates was estimated to be the highest by SEC with the vertical drop method (2.62%), followed by SEC with the Gaussian skim approach (2.54%), and AUC-SV (2.25%; Table 1).

The C(*s*) distribution of Tetanobulin showed two peaks corresponding to the monomeric and dimeric forms of the antibody (Fig. 1H). The amount of dimeric aggregates derived from the AUC-SV analysis was lower than the value obtained using the vertical drop method for chromatographic data analysis (Table 1). The SEC analysis detected a minor peak in the chromatogram corresponding to trimer/higher aggregates, which was not detected by AUC-SV (Fig. 1K). Integration of the chromatographic peaks showed that these species were present at amounts below the estimated limit of AUC-SV detection of 0.2% (25). Moreover, the obtained value was close to the limit of detection previously determined for SEC (TSK gel SEC Brochure – Tosoh Bioscience GmbH).

Aggregation analysis of lyophilized immunoglobulin preparations The two major peaks corresponding to the monomeric and dimeric forms of the antibody were detected by SEC and AUC-SV analyses of the Glovenin formulation. In the chromatogram (Fig. 1I), these peaks co-eluted and were baseline-unresolved. From integration of the chromatogram by using the vertical drop method, the amount of dimeric aggregates was estimated to be 1.18% higher compared with the estimate produced by the Gaussian skim integration algorithm and 1.39% higher compared with the estimate determined by the C(*s*) analysis of the AUC-SV data.

The chromatographic profile obtained for Gammagard indicated the presence of four major peaks corresponding to solvent, monomeric, dimeric, and trimeric forms of the antibody. The AUC-SV analysis also detected albumin and trace amounts of high-molecular weight aggregates. The amount of dimeric aggregates estimated by the vertical drop method of SEC chromatogram was significantly higher compared with that calculated using the Gaussian skim algorithm. However, the Gaussian skim algorithm failed to accurately resolve a minor peak corresponding to solvent preventing accurate quantification of the monomeric form of the antibody (Table 1).

There was a significant difference between the AUC-SV and SEC results obtained for Sanglopor independent of the integration approach applied to the SEC data analysis. Similar to other immunoglobulin preparations, the dimeric aggregates amount determined by the Gaussian skim algorithm was lower than that obtained by the vertical drop method. It is interesting that the amount of dimeric aggregates estimated by AUC-SV was lower than that calculated using the vertical drop method but was higher than that resulting from integration using the Gaussian skim approach. The AUC-SV analysis revealed the presence of two antibody fragments and trace amounts of high-molecular weight aggregates, which were not detected in the elution profile.

DISCUSSION

In the present study, the aggregate compositions of different preparations of human immunoglobulins were analyzed using AUC-SV and SEC with the vertical drop method and the Gaussian skim approach. Although AUC-SV and SEC degrees of precision differed, these two analytical techniques provided similar results in the quantification of aggregates confirming the complementary relationship between AUC-SV and SEC. As has been discussed (6,14,16,17), both SEC and AUC-SV methods can be used to quantify the aggregates in the pharmaceutical formulations. Due to its simplicity, speed, and reproducibility of obtained results, SEC is routinely used as a quality control method to evaluate the aggregation of pharmaceuticals. In contrast to SEC, AUC-SV does not conform to the requirements specified for the quality control methods because of the relatively low precision and repeatability. However, AUC-SV offers a significant advantage over SEC as it provides matrix-free separation of the solutes, and therefore, it can be performed to ensure that the sample's composition has not changed owing to interaction with the column packing material. In addition, larger soluble aggregates eluted in the void volume of the SEC column can be detected and characterized by AUC-SV (14).

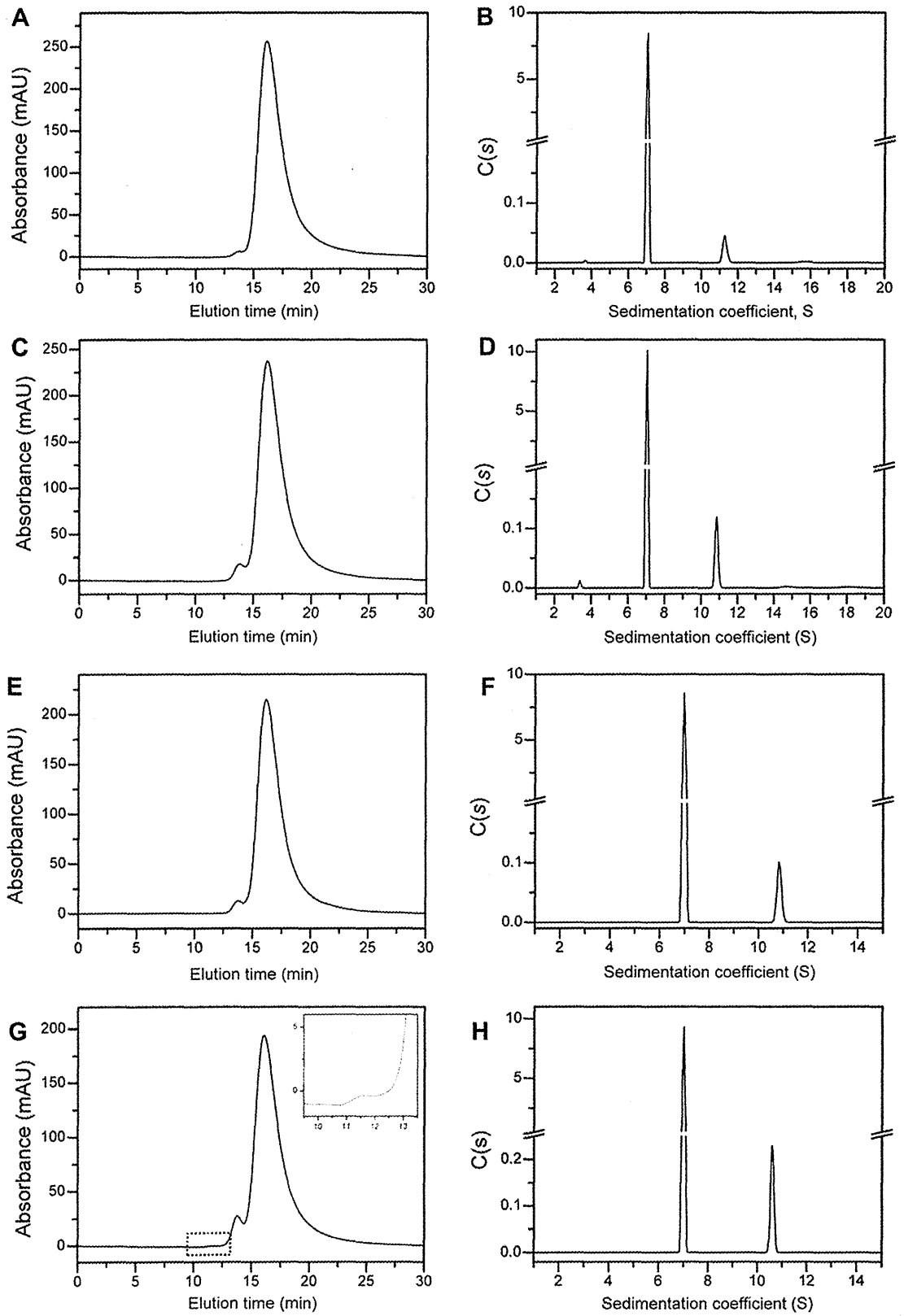

FIG. 1. Size-exclusion chromatograms and sedimentation coefficients distributions C(*s*) obtained for the following human immunoglobulin preparations: (A, B) Polyglobin, (C, D) Venoglobulin, (E, F) Hebsbulin, (G, H) Tetanobulin, (I, J) Glovenin, (K, L) Gammagard, and (M, N) Sanglopor. The insets in panels G and K show enlarged view of the boxed areas. The insets in panels L and N show the C(*s*) distributions with expanded vertical scale. The size-exclusion chromatograms and the continuous sedimentation coefficient distributions C(*s*) consistently showed the same number of peaks, with the exception of Sanglopor, for which the C(*s*) distribution indicated the presence of two peaks corresponding to antibody fragments, whereas these peaks were not seen in the SEC chromatogram.

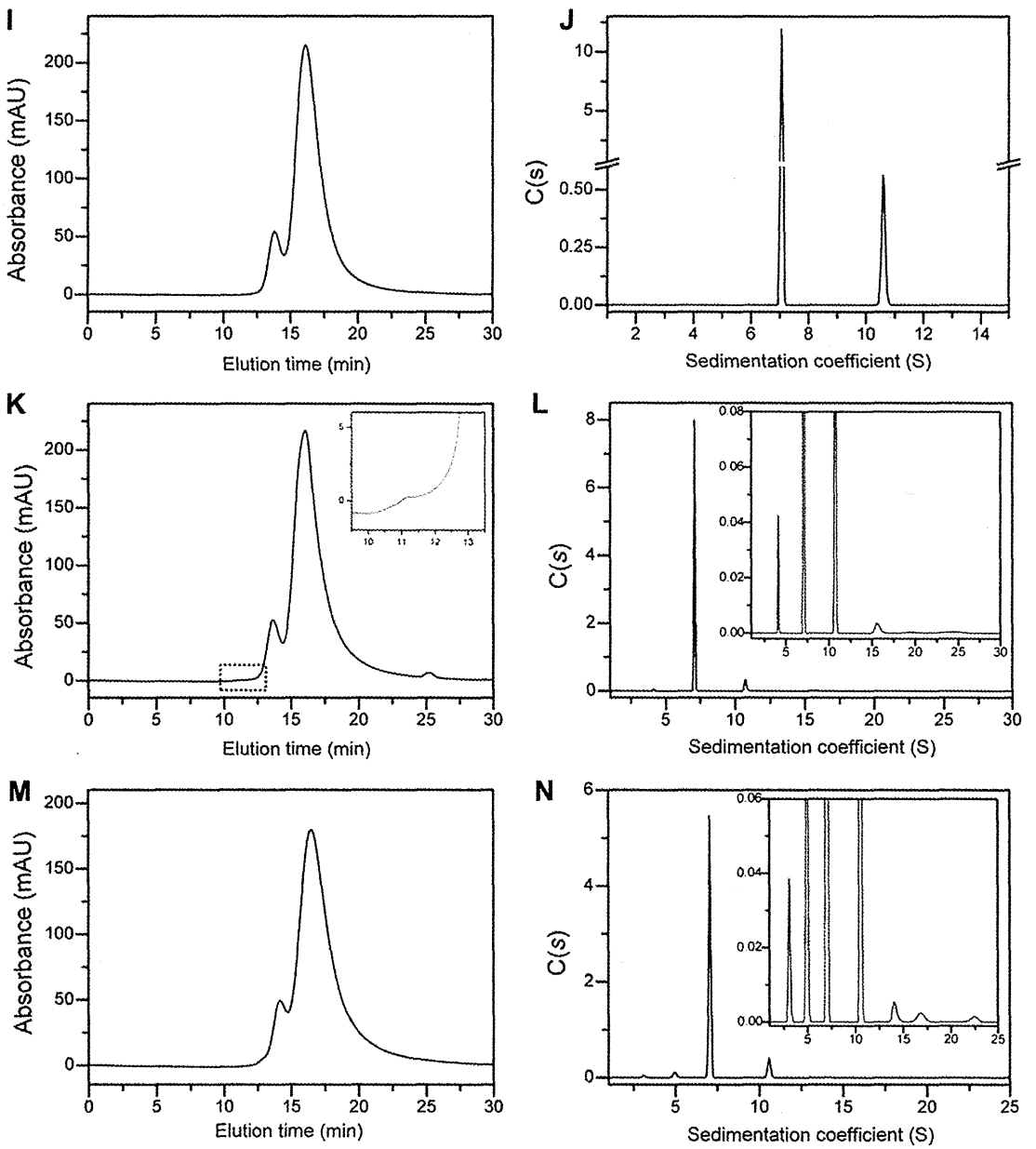

FIG. 1. (*continued*).

The results of the chromatographic analyses obtained using different integration approaches showed minimal variability for the solutions of Venoglobulin, Polyglobin, and Hebsbulin. For the other formulations used in this study, integration of the peaks using the vertical drop method systematically provided higher values of dimeric aggregate compared with those from the Gaussian skim approach. It was noted that with increase in the height of the valley between the unresolved peaks corresponding to monomer and dimer, the differences between estimates produced by the vertical drop method and the Gaussian integration approach increased. These differences were attributed to the differences in integration algorithms, and it was suggested that the Gaussian skim approach was inherently more accurate for overlapping peak separation than the traditional, vertical drop method. This conclusion is also supported by the AUC-SV results that showed better agreement with the results obtained using the Gaussian skim method, but not with the vertical drop method. However, in the case of Gammagard, the Gaussian skim method failed to accurately estimate the area under the small peak corresponding to solvent (Table 1) preventing correct quantification of the monomeric form of the antibody. A reasonably accurate result was obtained when tangential skim (algorithm that performs valley-to-valley extrapolation) (5) was applied, which is known to perform well when it is used to skim a much smaller and narrower peak from the large parent peak. However, similar to the result of the vertical drop method, the amount of dimeric aggregates was overestimated when the tangential skim approach was used. The analysis of the Gammagard chromatogram was complicated by the fact that the peaks could not conform to a single mathematical model, and the asymmetry and further overlapping of the peaks increased the complexity of the chromatogram.

The best way to eliminate measurement error is to increase the resolution of the chromatogram to obtain baseline separated peaks.

TABLE 1. Detailed quantitative summary of the results obtained by C(s) SEDFIT analysis of the AUC-SV data and by the vertical drop method and Gaussian skim algorithm analysis of the SEC data.

Product	Method	Albumin, %	Fragment, %	Monomer, %	Dimer, %	Trimer, %	HMW, %
Polyglobin	AUC[a]	–	0.33 ± 0.17	98.26 ± 0.27	1.27 ± 0.16	0.19 ± 0.07	–
	SEC-vertical drop[b]	–	–	99.20 ± 0.01	0.80 ± 0.01	–	–
	SEC-Gaussian skim[b]	–	–	99.20 ± 0.03	0.80 ± 0.03	–	–
Venoglobulin	AUC[a]	–	0.14 ± 0.02	97.24 ± 0.21	2.60 ± 0.21	0.18 ± 0.07	–
	SEC-vertical drop[b]	–	–	97.32 ± 0.08	2.68 ± 0.08	–	–
	SEC-Gaussian skim[b]	–	–	97.46 ± 0.07	2.54 ± 0.07	–	–
Hebsbulin	AUC[a]	–	–	97.75 ± 0.20	2.25 ± 0.20	–	–
	SEC-vertical drop[b]	–	–	97.45 ± 0.04	2.56 ± 0.04	–	–
	SEC-Gaussian skim[b]	–	–	97.47 ± 0.02	2.54 ± 0.02	–	–
Tetanobulin	AUC[a]	–	–	95.74 ± 0.21	4.26 ± 0.21	–	–
	SEC-vertical drop[b]	–	–	94.75 ± 0.11	5.15 ± 0.10	0.10 ± 0.01	–
	SEC-Gaussian skim[b]	–	–	95.51 ± 0.06	4.35 ± 0.06	0.14 ± 0.00	–
Glovenin	AUC[c]	–	–	90.76 ± 0.20	9.24 ± 0.20	–	–
	SEC-vertical drop[b]	–	–	89.37 ± 0.16	10.63 ± 0.16	–	–
	SEC-Gaussian skim[b]	–	–	90.55 ± 0.02	9.45 ± 0.02	–	–
Gammagard	AUC[c]	0.53 ± 0.13	–	92.05 ± 0.28	6.86 ± 0.26	0.34 ± 0.11	0.22 ± 0.04
	SEC-vertical drop[b]	1.57 ± 0.00[d]	–	88.61 ± 0.20	9.75 ± 0.14	0.11 ± 0.01	–
	SEC-Gaussian skim[b]	6.25 ± 0.25[d]	–	85.02 ± 0.06	8.40 ± 0.30	0.32 ± 0.04	–
Sanglopor	AUC[c]	–	1.07 ± 0.08 3.02 ± 0.26	85.40 ± 0.09	9.64 ± 0.09	0.47 ± 0.17	0.41 ± 0.02
	SEC-vertical drop[b]	–	–	89.69 ± 0.28	10.32 ± 0.28	–	–
	SEC-Gaussian skim[b]	–	–	91.34 ± 0.04	8.66 ± 0.04	–	–

[a] The data are the mean values of six measurements performed in three independent runs ± SD.
[b] The data are the mean values of triplicate measurements ± SD.
[c] The data are the mean values of two measurements performed in one run ± SD.
[d] The albumin peak was not detected. The reported value is the result of the solvent peak integration.

In general, this can be achieved by modifications of the mobile phase. However, the choice of optimum mobile phase is a tradeoff between resolution and accuracy. As has been discussed (6,22), adjustments of the mobile phase can increase the resolution and at the same time may affect the original aggregate distribution in the antibody formulation. In addition, by increasing the resolution between monomer and dimer, the resolution of higher oligomers can significantly be altered.

AUC-SV was extensively used for the characterization of antibody samples (16) and, in particular, was successfully applied to the aggregation analysis of pharmaceutical antibodies (20). In the present study, a very high degree of agreement was observed between AUC-SV and SEC results for liquid formulations of immunoglobulin. In contrast, the agreement was relatively poor in the case of reconstituted preparations. In these formulations, SEC measurements performed on consecutive days suggested the loss of monomer due to formation of dimeric aggregates. This process was shown to be relatively slow compared with the time course of the sedimentation experiment. Surprisingly, the amount of dimeric aggregates estimated using AUC-SV was lower than the value obtained by SEC. We concluded that in the reconstituted formulations used for the AUC-SV measurements, the equilibrium of the monomer–dimer reaction was shifted toward monomer formation owing to a hundred-fold dilution required to analyze these solutions.

In the case of Sanglopor, the AUC-SV analysis detected the presence of two fragments, which were not visible in the chromatogram (Fig. 1M). It is suggested that the highly asymmetrical large monomer peak eluted before the smaller fragments' peaks caused this effect. Another hypothesis was that the relatively long centrifugation times could cause the degradation of monomer into antibody fragments.

In conclusion, the results of AUC-SV and SEC were consistent and the degree of agreement was higher when the chromatographic data were analyzed by using the Gaussian skim approach (Fig. 2). Thus, the results of this study confirmed that AUC-SV is an appropriate complementary to SEC method for aggregate composition analysis and underscored the important role that the different integration methods can play in the quantitative interpretation of chromatographic results.

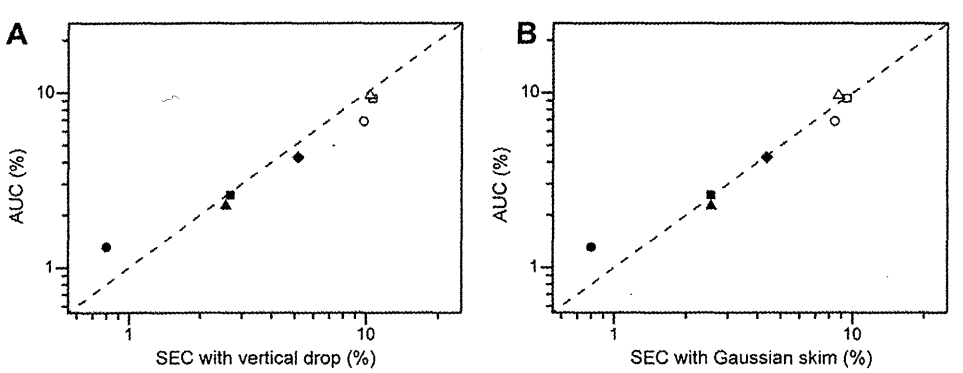

FIG. 2. Comparison of the dimeric aggregate amounts detected using AUC-SV and SEC with either (A) the vertical drop method or (B) the Gaussian skim approach. In each panel, the results for Polyglobin (filled circle), Venoglobulin (filled square), Hebsbulin (filled triangle), Tetanobulin (filled diamond), Gammagard (open circle), Sanglopor (open triangle), and Glovenin (open square) are shown. The degree of agreement between the AUC-SV and SEC results was higher when the Gaussian skim approach was applied for the chromatographic data analysis.

References

1. **Rosenberg, A. S.:** Effects of protein aggregates: an immunologic perspective, AAPS J., **8**, E501–E507 (2006).
2. **Meyer, V. R.:** Errors in the area determination of incompletely resolved chromatographic peaks, J. Chromatogr. Sci., **33**, 26–33 (1995).
3. **Foley, J. P.:** Systematic errors in the measurement of peak area and peak height for overlapping peaks, J. Chromatogr., **384**, 301–313 (1987).
4. **Meyer, V. R.:** Practical high-performance liquid chromatography, 5th ed., pp. 300–302. John Wiley & Sons, Ltd, UK (2010).
5. **Dyson, N.:** Chromatographic integration methods, 2nd ed., pp. 60–77. Royal Society of Chemistry, UK (1998).
6. **Arakawa, T., Ejima, D., Li, T., and Philo, J. S.:** The critical role of mobile phase composition in size exclusion chromatography of protein pharmaceuticals, J. Pharm. Sci., **99**, 1674–1692 (2010).
7. **Carpenter, J. F., Randolph, T. W., Jiskoot, W., Crommelin, D. J. A., Middaugh, C. R., and Winter, G.:** Potential inaccurate quantitation and sizing of protein aggregates by size exclusion chromatography: essential need to use orthogonal methods to assure the quality of therapeutic protein products, J. Pharm. Sci., **99**, 2200–2208 (2010).
8. **Berkowitz, S. A.:** Role of analytical ultracentrifugation in assessing the aggregation of protein biopharmaceuticals, AAPS J., **8**, E590–E605 (2006).
9. **Schuck, P.:** Diffusion-deconvoluted sedimentation coefficient distributions for the analysis of interacting and non-interacting protein mixtures, pp. 26–50, in: Scott, D. J., Harding, S. E., and Rowe, A. J. (Eds.), Analytical ultracentrifugation: techniques and methods. RSC Publishing, UK (2005).
10. **Harding, S. E.:** Analysis of polysaccharide size, shape and interactions, pp. 231–252, in: Scott, D. J., Harding, S. E., and Rowe, A. J. (Eds.), Analytical ultracentrifugation: techniques and methods. RSC Publishing, UK (2005).
11. **Demeler, B., Brookes, E., Wang, R., Schirf, V., and Kim, C. A.:** Characterization of reversible associations by sedimentation velocity with UltraScan, Macromol. Biosci., **10**, 775–782 (2010).
12. **Cole, J. L., Correia, J. J., and Stafford, W. F.:** The use of analytical sedimentation velocity to extract thermodynamic linkage, Biophys. Chem., **159**, 120–128 (2011).
13. **Arakawa, T., Philo, J. S., Ejima, D., Tsumoto, K., and Arisaka, F.:** Aggregation analysis of therapeutic proteins, Part 2: analytical ultracentrifugation and dynamic light scattering, Bioprocess Int., **5**, 36–47 (2007).
14. **Gabrielson, J. P., Brader, M. L., Pekar, A. H., Mathis, K. B., Winter, G., Carpenter, J. F., and Randolph, T. W.:** Quantitation of aggregate levels in a recombinant humanized monoclonal antibody formulation by size-exclusion chromatography, asymmetrical flow field flow fractionation, and sedimentation velocity, J. Pharm. Sci., **96**, 268–279 (2007).
15. **Liu, J., Andya, J. D., and Shire, S. J.:** A critical review of analytical ultracentrifugation and field flow fractionation methods for measuring protein aggregation, AAPS J., **22**, E580–E589 (2006).
16. **Philo, J. S.:** A critical review of methods for size characterization of non-particulate protein aggregates, Curr. Pharm. Biotechnol., **10**, 359–372 (2009).
17. **den Engelsman, J., Garidel, P., Smulders, R., Koll, H., Smith, B., Bassarab, S., Seidl, A., Hainzl, O., and Jiskoot, W.:** Strategies for the assessment of protein aggregates in pharmaceutical biotech product development, Pharm. Res., **28**, 920–933 (2011).
18. **Pekar, A. and Sukumar, M.:** Quantitation of aggregates in therapeutic proteins using sedimentation velocity analytical ultracentrifugation: practical considerations that affect precision and accuracy, Anal. Biochem., **367**, 225–237 (2007).
19. **Gabrielson, J. P., Arthur, K. K., Stoner, M. R., Winn, B. C., Kendrick, B. S., Razinkov, V., Svitel, J., Jiang, Y., Voelker, P. J., Fernandes, C. A., and Ridgeway, R.:** Precision of protein aggregation measurements by sedimentation velocity analytical ultracentrifugation in biopharmaceutical applications, Anal. Biochem., **396**, 231–241 (2010).
20. **Gabrielson, J. P. and Arthur, K. K.:** Measuring low levels of protein aggregation by sedimentation velocity, Methods, **54**, 83–91 (2011).
21. **Krayukhina, E., Uchiyama, S., and Fukui, K.:** Effects of rotational speed on the hydrodynamic properties of pharmaceutical antibodies measured by analytical ultracentrifugation sedimentation velocity, Eur. J. Pharm. Sci., **47**, 367–374 (2012).
22. **Philo, J. S.:** Is any measurement method optimal for all aggregate sizes and types? AAPS J., **8**, E564–E571 (2006).
23. **Eberlein, G. A.:** Quantitation of proteins using HPLC-detector response rather than standard curve comparison, J. Pharm. Biomed. Anal., **13**, 1263–1271 (1995).
24. **Schuck, P.:** Size-distribution analysis of macromolecules by sedimentation velocity ultracentrifugation and Lamm equation modeling, Biophys. J., **78**, 1606–1619 (2000).
25. **Brown, P. H., Balbo, A., and Schuck, P.:** A Bayesian approach for quantifying trace amounts of antibody aggregates by sedimentation velocity analytical ultracentrifugation, AAPS J., **10**, 481–493 (2008).

Biochemical and Biophysical Research Communications 424 (2012) 519–523

Contents lists available at SciVerse ScienceDirect

Biochemical and Biophysical Research Communications

journal homepage: www.elsevier.com/locate/ybbrc

Toll-like receptor (TLR) 3 as a surrogate sensor of retroviral infection in human cells

Kosuke Miyauchi [a,d], Emiko Urano [a], Satoshi Takeda [a], Tsutomu Murakami [a], Yoshiaki Okada [b], Kui Cheng [c], Hang Yin [c], Masato Kubo [d,e], Jun Komano [a,*]

[a] AIDS Research Center, National Institute of Infectious Diseases, 1-23-1 Toyama, Shinjuku, Tokyo 162-8640, Japan
[b] Division of Safety Research on Blood and Biological Products, National Institute of Infectious Diseases, 4-7-1 Murayama, Tokyo 208-0011, Japan
[c] Department of Chemistry and Biochemistry, University of Colorado at Boulder, Boulder, CO 80309-0215, United States
[d] Research Center for Allergy and Immunology, RIKEN Yokohama Institute, 1-7-22 Suehiro-cho, Tsurumi, Yokohama, Kanagawa 230-0045, Japan
[e] Division of Molecular Pathology, Research Institute for Biological Sciences, Tokyo University of Sciences, 2669 Yamazaki, Noda, Chiba 278-0022, Japan

ARTICLE INFO

Article history:
Received 20 June 2012
Available online 4 July 2012

Keywords:
Human
Cytokines
Signal Transduction
Viral infections (major category)
Toll-like receptor (TLR)
Retrovirus
Interferon gamma-induced protein 10 (IP-10)/CXCL10

ABSTRACT

The toll-like receptor (TLR)-7 has been shown to sense the retroviral infection. However, a surrogate sensor has been implicated. We examined whether retrovirus serves as a TLR3 ligand in human cells by utilizing cell lines LNCaP and PC-3 lacking TLR7, and the xenotropic murine leukemia virus-relamoted virus (XMRV) insensitive to human tripartite motif-containing (TRIM) 5, a newly characterized pattern recognition receptor (PRR). A dominant-negative TLR3 or a chemical inhibitor of TLR3 attenuated the XMRV-induced IP-10/CXCL10 expression, a marker of TLR3 response. These data clearly indicated that retroviral infection exemplified by XMRV activates the TLR3 signal in human cells.

1. Introduction

The pattern recognition receptor (PRR) plays a key role in the innate immune response to microbial infection [1,2]. Viral RNA can serve as a ligand for the PRR system. Such RNA sensors are present in both endosomes (for example, toll-like receptor (TLR)-3 and -7, double and single-stranded RNA sensors, respectively) and cytoplasm (for example, retinoic acid-inducible gene-I, RIG-I; melanoma differentiation associated gene-5, MDA5). TLR3 is also known to be expressed on the cell surface of epithelial origin [3]. The use of RNA sensors in host defense against retroviral infection remains controversial.

Retroviruses are enveloped viruses with single-stranded RNA genomes. Retroviruses replicate using a unique strategy to protect the viral genomic RNA from being recognized by host RNA sensors. In the production phase of the retroviral life cycle, transcription from proviral DNA integrated into the host chromosome occurs via a mechanism that is essentially identical to that of transcription of cellular genes. The accumulation levels of viral transcript in the infected cells are modest relative to other RNA viruses encoding their own RNA polymerases to amplify viral RNA. In this sense, the mRNA of proviral DNA is barely distinguishable from mRNA transcribed from cellular genes unless the viral RNA has some sequences that evoke anti-viral responses [4,5], which does not apply to all the retroviral species. No evidence has been reported whether the TLR3/7-mediated signal is activated by retroviral RNA transcribed from the provirus. The retroviral genome is not exposed to the surface of virion. Thus, the recognition of retroviral genomic RNA at the cell surface appears unlikely. In the entry phase, the viral genome released into the cytoplasm after the virus-cell membrane fusion is packed in the core. The reverse transcription of viral genome takes place in the cytoplasm and the reverse-transcribed viral DNA is mostly covered with proteins forming the preintegration complex (PIC) [6]. Thus, the exposure of viral genome to the cytoplasmic viral RNA sensor appears limited. Thus, the reverse-transcribed viral DNA may not serve as an efficient ligand for cytoplasmic DNA sensors, such as the DNA-dependent activator of interferon regulatory factor (DAI).

A fraction of retroviral particles, either infectious or non-infectious, are actively endocytosed and degraded in the endosome/lysosome, providing the viral genome as a ligand for RNA sensors, namely a single-stranded RNA sensor TLR7 [7–11]. This model has been tested directly in dendritic cell/human immunodeficiency

Abbreviations: AZT, azidothymidine; dnTLR, dominant negative TLR; PIC, preintegration complex; TRIM, tripartite motif-containing.

* Corresponding author. Address: Osaka Prefectural Institute of Public Health, Dept. of Infectious Diseases, Virology Division, 3-69, Nakamachi, 1-chome, Higashinari-ku, Osaka 537-0025, Japan. Fax: +81-6-6972-2393.
E-mail addresses: ajkomano@nih.go.jp, komano@iph.pref.osaka.jp (J. Komano).

0006-291X/$ - see front matter © 2012 Elsevier Inc. All rights reserved.
http://dx.doi.org/10.1016/j.bbrc.2012.06.148

virus type 1 (HIV-1) systems [7]. Human T-cell luekemia virus type 1 (HTLV-1) has been also shown to activate TLR7-mediated signal [12]. Not only TLR7, TLR8 and TLR9 have been involved in the recognition of retroviruses [7,9]. Interestingly, the retroviral infection still evokes some host immune response in the absence of TLR7, suggesting a surrogate sensor of retroviral infection [7,9,10]. It has been reported that HIV-based lentiviral vectors evoke signals from TLR3 as well as TLR7 in mouse cells [1]. However, the involvement of TLR3 in the recognition of infecting retroviral genomes remains to be clarified in human cells.

The retroviral genome is predicted to dimerize and form an extensive secondary structure [13–15]. In these processes, it is likely that double-stranded RNA, a ligand of TLR3, is formed. We hypothesized that retroviruses can potentially activate TLR3 during the viral entry phase. In this study, we demonstrated definitively that TLR3 is a sensor of retroviral genome in human cells through a genetic and a chemical biology approaches.

2. Materials and methods

2.1. Tissue culture

Cells were maintained in RPMI 1640 medium (Sigma, St. Louis, MO) supplemented with 10% fetal bovine serum (Japan Bioserum, Tokyo, Japan), 50 U/ml penicillin and 50 μg/ml streptomycin (Invitrogen, Tokyo, Japan) at 37 °C in a humidified 5% CO_2 atmosphere. 22RV-1 and LNCaP (clone FGC) were obtained from Dainippon Sumitomo Pharma Biomedical (Osaka, Japan), while PC-3 and DU145 were obtained from the National Institute of Radiological Sciences. AZT was obtained from the NIH AIDS Research and Reference Reagent Program. The TLR3 ligand, poly(I:C12U), was used at a concentration of 25 μg/ml (Hemispherx Biopharma, Philadelphia, PA). Imiquimod (Sigma) was used at a concentration of 40 μM. The TLR3 inhibitor 4a has been described previously [16].

2.2. Cytokine measurement

The levels of IP-10/CXCL10 were measured using Quantikine IP-10 ELISA kit for the most of the data (R&D Systems, Minneapolis, MN), except 23-Plex panel of the Bioplex cytokine assay system was used for the experiment in Fig. 1D (Bio-Rad Laboratories, Hercules, CA).

2.3. Virus

The xenotropic murine leukemia virus-relamoted virus (XMRV) was prepared from the tissue culture supernatant of 22RV-1 cells. Tissue culture supernatants of 22RV-1 cells were passed through nitrocellulose filters (0.45 μm) and the virions were collected by centrifugation over 20% (w/w) sucrose/PBS (Optima™ L-70 k, SW 55 Ti rotor, 11 k × *g* for 2 h; Beckman Coulter, Miami, FL). The pellet was resuspended in tissue culture medium to 1/10–20 the original volume. Approximately 5% of LNCaP cells were infected with XMRV at 2 days-postinfection as determined by immunofluorescent assay using anti-R-MuLV p30 (Gag) polyclonal serum (NCI BCB repository, 81S263). The MuLV vector was produced as described previously [17]. Replication of XMRV was measured by assessing RT acitivity using the EnzChek Reverse Transcriptase Assay kit (Invitrogen).

2.4. Western blotting

Western blotting was performed as described previously [18]. The following probes were used: an anti-hemagglutinin (HA) monoclonal antibody 6E2 (Cell Signaling Technology, Beverly, MA); an anti-actin monoclonal antibody 1501R (Millipore); and a biotin conjugated secondary antibody and streptavidin conjugated with horseradish peroxidase (HRP, GE Healthcare, Tokyo, Japan).

2.5. RT-PCR

Total RNA from LNCaP cells was isolated using the SV Total RNA Isolation System (Promega, Madison, WI). RT-PCR was carried out using the OneStep RT-PCR Kit (Qiagen, Valencia, CA) using the following primers: TLR3, 5′-TGG TTG GGC CAC CTA GAA GTA-3′ and 5′-TCT CCA TTC CTG GCC TGT G-3′; TLR7, 5′-TTT ACC TGG ATG GAA ACC AGC TA-3′ and 5′-TCA AGG CTG AGA AGC TGT AAG CTA-3′; IP-10/CXCL10, 5′-TTC AAG GAG TAC CTC TCT CTA G-3′ and 5′-CTG GAT TCA GAC ATC TCT TCT C-3′; GAPDH for Fig. 1A, 5′-GTG GAA GGA CTC ATG ACC ACA GTC-3′ and 5′-CAT GTG GGC CAT GAG GTC CAC CAC-3′; and GAPDH for Fig. 2B, 5′-GTC GGA GTC AAG GAT TTG-3′ and 5′-TGG TGG AAT CAT ATT GGA A-3′.

2.6. Cloning

The cDNA library of human PBMCs was used as a template (Takara, Otsu, Japan). The following primers were used: forward, 5′-AGC GGC CGC ACC ATG AGA CAG ACT TTG CCT TGT ATC TAC TTT TGG-3′ and reverse, 5′-AAC CGG TTA GGC GTA GTC TGG CAC ATC ATA GGG GTA AAA CTG TTC TGT CTG TCT GTC TAT TTC TTT G-3′. The reverse primer contained the HA tag sequence. The PCR fragment spanning the ectodomain and transmembrane domain of tlr3 was cloned into NotI-AgeI sites of pQcXIP (Clontech, Palo Alto, CA). The pQcXIP without an insert was used as a control for pQcdnTLR3. The LNCaP cells were infected with the MuLV vector and selected with 1.0 μg/ml puromycin.

3. Results and discussion

To clearly differentiate the TLR3 signal from TLR7 in human cells, we carefully chose the experimental system. The prostate cancer cell lines LNCaP and PC-3 have been chosen for cells because they expressed TLR3 endogenously but not TLR7 [19]. We verified the lack of TLR7 expression by RT-PCR in these cell lines in agreement with the previous report (Fig. 1A) [19]. We chose XMRV because this retrovirus is not restricted by a newly-identified PRR protein human tripartite motif-containing (TRIM) 5 [20–22]. The exposure of LNCaP cells to bacteria-derived plasmid DNA induced the robust production of a PRR-responsive cytokine, namely interferon gamma-induced protein 10 (IP-10)/CXCL10. Thus, the viral vectors were not suitable for this study since the complete removal of plasmids or bacteria-derived contaminants from the preparation of viral vectors was difficult [23]. The advantage of XMRV is that the plasmid-free viral preparation is achievable using 22RV-1 cells latently infected with XMRV [24]. The mouse mammary tumor virus (MMTV) activates the signal from TLR4 that targets non-nucleic acid components [25]. The signals from TLR7, 8, and 9 have been activated by retroviruses [7–12]. Another advantage of using the LNCaP-XMRV system is that LNCaP cells do not express TLR4, 8 and 9, in addition to TLR7 [19]. Furthermore, RNase L and JAK in LNCaP cells are defective, both are involved in the interferon (IFN)-mediated anti-viral responses [26–29]. Thus, the signal we detected was not due to any retroviral sensors identified thus far that target non-nucleic acid components. We chose IP-10/CXCL10, one of the PRR-inducible cytokines, as a marker to monitor the cellular response toward TLR3 ligand according to Galli et al. [19] for the induction of IP-10/CXCL10 by TLR3 ligand was reproducible (Fig. 1B). The replication kinetics of XMRV were measured in relation to the production of IP-10/CXCL10. The IP-10/CXCL10 production profile was almost identical

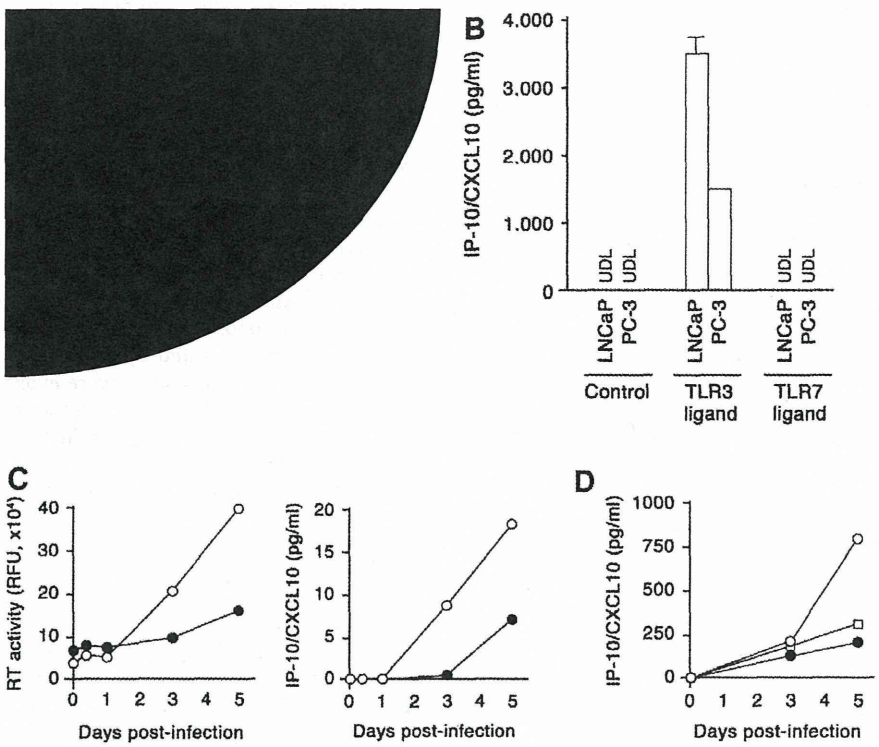

Fig. 1. Expression profiling of TLR3/7 and IP-10/CXCL10 in prostate cancer cell lines. (A) Verification of TLR3 expression in LNCaP, PC-3, and DU-145 cell but not TLR7 by RT-PCR. Total RNA isolated from peripheral blood mononucler cells (PBMC) was used as a positive control. (B) Production of IP-10/CXCL10 in response to TLR3 and TLR7 ligands. LNCaP and PC-3 cells were exposed to TLR3 ligand or TLR7 ligand for 5 days, and the tissue culture supernatants were examined by ELISA. The control is solvent only (PBS and DMSO for TLR3 and TLR7 ligands, respectively). The error bar represents the SD of triplicated wells. Representative data from three independent experiments are shown. UDL, under the detection limit. (C) Correlation of XMRV replication and IP-10/CXCL10 production kinetics in LNCaP cells. The culture supernatant was subjected to RT assay (left) and IP10/CXCL10 ELISA (right). For the control, the replication of XMRV was inhibited by 5 μM AZT (filled). Representative data from three independent experiments are shown. RFU, relative fluorescent units. (D) Induction of IP-10/CXCL10 by XMRV infection in PC-3 cells. Cells were infected with XMRV and maintained in the absence (open circle) or presence (filled circle) of AZT. The MOCK control was also shown (open rectangle).

to the replication profile of XMRV (Fig. 1C). The production of IP-10/CXCL10 from LNCaP cells was reduced when XMRV replication was inhibited by azidothymidine (AZT). Similar results were obtained in PC-3 cells (Fig. 1D). The upregulation of IP-10/CXCL10 was at the transcriptional levels as demonstrated below. These data indicate that XMRV replication induces the expression of IP-10/CXCL10 under the TLR7-null conditions. Note that the IP-10/CXCL10 levels in TLR3 ligand-exposed LNCaP cells were higher than those in XMRV-infected cells (Fig. 1B v.s. Fig. 1C). This is likely because almost all the cells were fully activated by the TLR3 ligand, whereas XMRV infection was limited to a portion of cells.

We then asked whether TLR3 is responsible for these responses. The specific involvement of TLR3 in the upregulation of IP-10/CXCL10 by XMRV infection was investigated by both genetic and chemical approaches. The RNA silencing approach was not employed because siRNA/shRNA potentially serves as a TLR3 ligand [3,30]. First, a dominant-negative derivative of TLR3 (dnTLR3) [31], devoid of cytoplasmic Toll/IL-1 receptor (TIR) domain required for TLR3 signaling, was transduced into LNCaP cells by a murine leukemia virus (MuLV) vector. We verified dnTLR3 expression in LNCaP cells by Western blot analysis where the dnTLR3 was tagged with a HA epitope tag (Fig. 2A). The baseline of the IP-10/CXCL10 production levels was increased in puromycin-selected LNCaP cells. It was assumed that puromycin triggers production of IP-10/CXCL10 since the removal of puromycin from the culture medium reduced the IP-10/CXCL10 levels (data not shown). The control cells responded to both TLR3 ligand and XMRV infection to produce IP-10/CXCL10 (Fig. 2A). In contrast, both XMRV infection and the TLR3 ligand did not upregulate the expression of IP-10/CXCL10 in LNCaP/dnTLR3 cells (Fig. 2A). Second, we treated LNCaP cells with a TLR3 inhibitor and infected cells with XMRV [16]. RT-PCR was employed to examine whether the induction of IP-10/CXCL10 by XMRV infection was at the transcriptional level. Under the conditions whereby the solvent control did not affect the induction of IP-10/CXCL10 by XMRV infection, TLR3 inhibitor was shown to limit the induction of IP-10/CXCL10 by XMRV infection from LNCaP cells (Fig. 2B). The inhibition of IP-10/CXCL10 induction by XMRV was dose-dependent (Fig. 2B). These data suggest that the induction of IP-10/CXCL10 by XMRV infection occurs at the transcriptional level. Taken together, it is suggested that TLR3 is responsible for the recognition of XMRV to induce production of IP-10/CXCL10.

It has been reported that HIV-1 activates TLR7-mediated signals but the contribution of TLR3, a double-stranded RNA sensor in the endosome and on the cell surface, in the anti-retroviral response has remained elusive [7–11]. We demonstrated that not only TLR7 but also TLR3 is able to recognize the retroviral genome and evokes an anti-viral response using XMRV as a model. Retrovirus has a single-stranded RNA as a genome. The retroviral RNA is predicted to form a higher order structure by base-pairing [13–15]. Thus, a portion of retroviral RNA should be able to serve as a TLR3 ligand. Although XMRV was employed in this experiment, it is likely that the recognition of retroviral genome via TLR3 applies to retroviruses in general, including HIV-1. We favor the model that XMRV activates TLR3 signaling at the endosomes given that a similar mechanism has been implicated in the recognition of HIV-1 and HTLV-1 by TLR7 [8,9,11,12]. XMRV has been shown to enter cells via endocytosis [32]. However, some viruses may fail

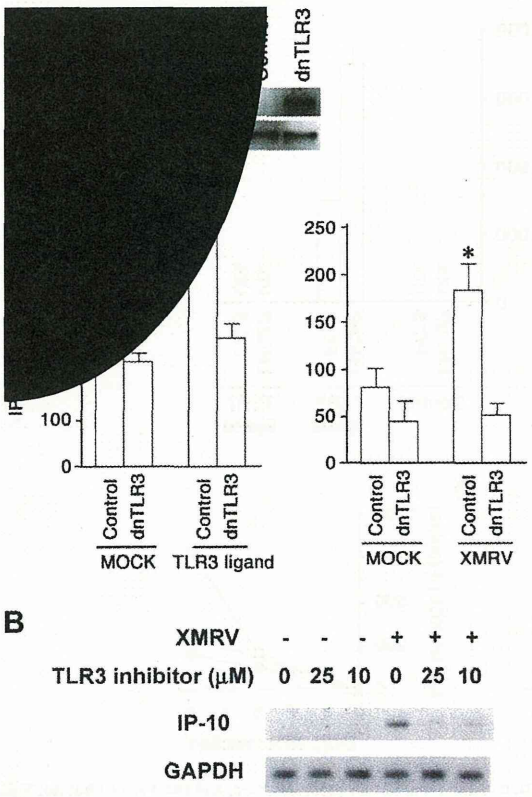

Fig. 2. Specific contribution of TLR3 to XMRV-induced IP-10/CXCL10. (A) Inhibition of IP-10/CXCL10 production by a dominant-negative derivative of TLR3 (dnTLR3). The dnTLR3 was transduced into LNCaP cells by MuLV vector and the cells were selected with puromycin. The constitutive expression of dnTLR3 in LNCaP cells was verified by Western blot analysis (upper panel). Actin was used as the internal control. The TLR3 ligand and XMRV infection failed to upregulate production of IP-10/CXCL10 by cells expressing dnTLR3 (lower panel). The error bar represents the SD of triplicated wells. Representative data from three independent experiments are shown. Statistical significance was detected between ligand-exposed or XMRV-infected control cells and each of the other groups by two-tailed Student's *t*-test (asterisk, $P < 0.01$). (B) Inhibition of XMRV-induced IP-10/CXCL10 production by a TLR3 inhibitor. The RNA isolated from LNCaP cells infected with XMRV in the presence or absence of the TLR3 inhibitor 4a (10 and 25 μM) was subjected to RT-PCR designed to detect IP-10/CXCL10 mRNA. GAPDH was used as the internal control. Representative data from three independent experiments are shown.

to infect cells because retroviruses are intrinsically unstable due to the loss of Env function [33]. Such defective viruses should be degraded in the endosome where the genomic RNA from these viral particles could be exposed to the host RNA sensors, including TLR3. The "endosome model" can be tested by using endosomal acidification inhibitors as reported by Beignon et al. [1]. However, this experimental approach was not possible in our experimental setting because IP-10/CXCL10 production was attenuated by such inhibitors, including Chloroquine or Bafilomycin A1. Retrovirus is an enveloped virus. Thus, the genomic RNA of XMRV should not be exposed to the surface of the virion. It appears unlikely, therefore, that the recognition of viral genomic RNA by TLR3 takes place at the cell surface unless TLR3 recognizes non-nucleic acid component on the surface of XMRV particle.

The historical studies on recognition of retroviruses by TLRs did not assess the involvement of a newly-identified PRR, TRIM5 [22]. In our experimental system, this potential caveat is clarified because human TRIM5 does not restrict XMRV entry [21,22]. The contribution of TLR3 to the recognition of retroviruses could have been difficult to detect partly because the expression levels of TLR7 might be higher than those of TLR3 in that experimental system, or that the TLR3-induced signal might not have been robust enough to detect. Thus, the failure of TLR3 signal detection does not necessarily mean that retroviruses do not activate the TLR3 signal. In the study by Breckpot et al. [34], activation of the TLR signal depended on reverse transcription of the viral genome using a replication-defective HIV-1-based lentiviral vector in mouse-derived dendritic cells. The reverse transcription of retroviral genome is considered to take place in the cell cytoplasm. Thus, the molecular sensor that recognizes the reverse-transcribed nucleic acid should be present in the cytoplasm, not in the endosomal compartment. The activation of anti-viral signal reported by Breckpot et al. should be, therefore, TLR3-independent. More recently, Kane et al. reported that MMTV and MuLV activate humoral responses via the TLR7 signal in mouse [10]. This, again, does not necessarily prove that TLR3 is not activated by these retroviruses, for it was noted that some immune responses were evoked by retroviral infection in a TLR7-independent manner. Although TLR7 serves as a front line, the TLR3 may be the second line PRR-mediated host defense against retroviruses. The *in vivo* relevance of TLR3 activation by retroviruses remains to be clarified in future studies.

Acknowledgments

K.M., E.U., S.T., T.M., Y.O., K.C., H.Y., M.K., and J.K. designed and performed the experiments and interpreted the data. J.K., E.U. and K.M. wrote the manuscript. This work was supported by the Japan Health Science Foundation, the Japanese Ministry of Health, Labor, and Welfare, and the Japanese Ministry of Education, Culture, Sports, Science and Technology. All authors declare no potential competing financial interests.

References

[1] K. Brennan, A.G. Bowie, Activation of host pattern recognition receptors by viruses, Curr. Opin. Microbiol. 13 (2010) 503–507.
[2] T. Kawai, S. Akira, The role of pattern-recognition receptors in innate immunity: update on Toll-like receptors, Nat. Immunol. 11 (2010) 373–384.
[3] M.E. Kleinman, K. Yamada, A. Takeda, et al., Sequence- and target-independent angiogenesis suppression by siRNA via TLR3, Nature 452 (2008) 591–597.
[4] X. Guo, J.W. Carroll, M.R. Macdonald, et al., The zinc finger antiviral protein directly binds to specific viral mRNAs through the CCCH zinc finger motifs, J. Virol. 78 (2004) 12781–12787.
[5] D. Wolf, S.P. Goff, Embryonic stem cells use ZFP809 to silence retroviral DNAs, Nature 458 (2009) 1201–1204.
[6] M.K. Lewinski, F.D. Bushman, Retroviral DNA integration–mechanism and consequences, Adv. Genet. 55 (2005) 147–181.
[7] A.S. Beignon, K. McKenna, M. Skoberne, et al., Endocytosis of HIV-1 activates plasmacytoid dendritic cells via Toll-like receptor-viral RNA interactions, J. Clin. Invest. 115 (2005) 3265–3275.
[8] A.W. Hardy, D.R. Graham, G.M. Shearer, et al., HIV turns plasmacytoid dendritic cells (pDC) into TRAIL-expressing killer pDC and down-regulates HIV coreceptors by Toll-like receptor 7-induced IFN-alpha, Proc. Natl. Acad. Sci. USA 104 (2007) 17453–17458.
[9] S.I. Gringhuis, M. van der Vlist, L.M. van den Berg, et al., HIV-1 exploits innate signaling by TLR8 and DC-SIGN for productive infection of dendritic cells, Nature 11 (2010) 419–426.
[10] M. Kane, L.K. Case, C. Wang, et al., Innate immune sensing of retroviral infection via toll-like receptor 7 occurs upon viral entry, Immunity 2011 (2011) 29.
[11] A. Lepelley, S. Louis, M. Sourisseau, et al., Innate sensing of HIV-infected cells, PLoS 7 (2011) e1001284.
[12] R. Colisson, L. Barblu, C. Gras, F. Raynaud, R. Hadj-Slimane, C. Pique, O. Hermine, Y. Lepelletier, J.P. Herbeuval, Free HTLV-1 induces TLR7-dependent innate immune response and TRAIL relocalization in killer plasmacytoid dendritic cells, Blood 115 (2010) 2177–2185.
[13] R.S. Russell, C. Liang, M.A. Wainberg, Is HIV-1 RNA dimerization a prerequisite for packaging? Yes, no, probably?, Retrovirology 1 (2004) 23.
[14] J. Greatorex, The retroviral RNA dimer linkage: different structures may reflect different roles, Retrovirology 1 (2004) 22.
[15] J.M. Watts, K.K. Dang, R.J. Gorelick, et al., Architecture and secondary structure of an entire HIV-1 RNA genome, Nature 460 (2009) 711–716.
[16] K. Cheng, X. Wang, H. Yin, Small-molecule inhibitors of the TLR3/dsRNA complex, J. Am. Chem. Soc. 133 (2011) 3764–3767.
[17] J. Komano, K. Miyauchi, Z. Matsuda, et al., Inhibiting the Arp2/3 complex limits infection of both intracellular mature vaccinia virus and primate lentiviruses, Mol. Biol. Cell 15 (2004) 5197–5207.

[18] S. Shimizu, E. Urano, Y. Futahashi, et al., Inhibiting lentiviral replication by HEXIM1, a cellular negative regulator of the CDK9/cyclin T complex, AIDS 21 (2007) 575–582.
[19] R. Galli, D. Starace, R. Busa, et al., TLR stimulation of prostate tumor cells induces chemokine-mediated recruitment of specific immune cell types, J. Immunol. 184 (2010) 6658–6669.
[20] M.J. Metzger, C.J. Holguin, R. Mendoza, A.D. Miller, et al., The prostate cancer-associated human retrovirus XMRV lacks direct transforming activity but can induce low rates of transformation in cultured cells, J. Virol. 84 (2010) 1874–1880.
[21] H.C. Groom, M.W. Yap, R.P. Galao, S.J. Neil, et al., Susceptibility of xenotropic murine leukemia virus-related virus (XMRV) to retroviral restriction factors, Proc. Natl. Acad. Sci. USA 107 (2010) 5166–5171.
[22] T. Pertel, S. Hausmann, D. Morger, S. Zuger, et al., TRIM5 is an innate immune sensor for the retrovirus capsid lattice, Nature 472 (2011) 361–365.
[23] A. Pichlmair, S.S. Diebold, S. Gschmeissner, et al., Tubulovesicular structures within vesicular stomatitis virus G protein-pseudotyped lentiviral vector preparations carry DNA and stimulate antiviral responses via Toll-like receptor 9, J. Virol. 81 (2007) 539–547.
[24] E.C. Knouf, M.J. Metzger, P.S. Mitchell, et al., Multiple integrated copies and high-level production of the human retrovirus XMRV (xenotropic murine leukemia virus-related virus) from 22Rv1 prostate carcinoma cells, J. Virol. 83 (2009) 7353–7356.
[25] D. Burzyn, J.C. Rassa, D. Kim, et al., Toll-like receptor 4-dependent activation of dendritic cells by a retrovirus, J. Virol. 78 (2004) 576–584.
[26] G.P. Dunn, K.C. Sheehan, L.J. Old, et al., IFN unresponsiveness in LNCaP cells due to the lack of JAK1 gene expression, Cancer Res. 65 (2005) 3447–3453.
[27] J.J. Rodriguez, S.P. Goff, Xenotropic murine leukemia virus-related virus establishes an efficient spreading infection and exhibits enhanced transcriptional activity in prostate carcinoma cells, J. Virol. 84 (2009) 2556–2562.
[28] B.P. Doehle, F. Hladik, J.P. McNevin, et al., Human immunodeficiency virus type 1 mediates global disruption of innate antiviral signaling and immune defenses within infected cells, J. Virol. 83 (2009) 10395–10405.
[29] S. Bhosle, S. Suppiah, R. Molinaro, et al., Evaluation of cellular determinants required for in vitro xenotropic murine leukemia virus-related virus entry into human prostate cancer and noncancerous cells, J. Virol. 84 (2010) 6288–6296.
[30] K. Kariko, P. Bhuyan, J. Capodici, et al., Small interfering RNAs mediate sequence-independent gene suppression and induce immune activation by signaling through toll-like receptor 3, J. Immunol. 172 (2004) 6545–6549.
[31] L. Alexopoulou, A.C. Holt, R. Medzhitov, et al., Recognition of double-stranded RNA and activation of NF-kappaB by Toll-like receptor 3, Nature 413 (2001) 732–738.
[32] H. Kamiyama, K. Kakoki, H. Yoshii, et al., Infection of XC cells by MLVs and Ebola virus is endosome-dependent but acidification-independent, PLoS One 6 (2011) e26180.
[33] S. Andreadis, T. Lavery, H.E. Davis, et al., Toward a more accurate quantitation of the activity of recombinant retroviruses: alternatives to titer and multiplicity of infection, J. Virol. 74 (2000) 3431–3439.
[34] K. Breckpot, D. Escors, F. Arce, et al., HIV-1 lentiviral vector immunogenicity is mediated by Toll-like receptor 3 (TLR3) and TLR7, J. Virol. 84 (2010) 5627–5636.

Transfusion and Apheresis Science 48 (2013) 95–102

Contents lists available at SciVerse ScienceDirect

Transfusion and Apheresis Science

journal homepage: www.elsevier.com/locate/transci

Online reporting system for transfusion-related adverse events to enhance recipient haemovigilance in Japan: A pilot study

Chikako Odaka [a], Hidefumi Kato [b], Hiroko Otsubo [a], Shigeru Takamoto [b], Yoshiaki Okada [a], Maiko Taneichi [a], Kazu Okuma [a], Kimitaka Sagawa [c], Yasutaka Hoshi [d], Tetsunori Tasaki [d], Yasuhiko Fujii [e], Yuji Yonemura [f], Noriaki Iwao [g], Asashi Tanaka [h], Hitoshi Okazaki [i], Shun-ya Momose [j], Junichi Kitazawa [k], Hiroshi Mori [l], Akio Matsushita [m], Hisako Nomura [n], Hitoshi Yasoshima [o], Yasushi Ohkusa [p], Kazunari Yamaguchi [a], Isao Hamaguchi [a,*]

[a] Department of Safety Research on Blood and Biological Products, National Institute of Infectious Diseases, Tokyo, Japan
[b] Department of Transfusion Medicine, Aichi Medical University, Aichi, Japan
[c] Department of Laboratory Medicine, Kurume University, Fukuoka, Japan
[d] Department of Transfusion Service, Tokyo Jikei University, Tokyo, Japan
[e] Department of Blood Transfusion, Yamaguchi University School of Medicine, Yamaguchi, Japan
[f] Department of Transfusion Medicine and Cell Therapy, Kumamoto University, Kumamoto, Japan
[g] Department of Transfusion Medicine and Cell Therapy, University of Yamanashi, Kumamoto, Japan
[h] Department of Blood Transfusion, Tokyo Medical University Hachioji Medical Center, Tokyo, Japan
[i] Central Blood Institute, Blood Service Headquarters, Japanese Red Cross Society, Tokyo, Japan
[j] Blood Service Headquarters, Japanese Red Cross Society, Tokyo, Japan
[k] Kuroishi General Hospital, Aomori, Japan
[l] Minami Tama Hospital, Tokyo, Japan
[m] Shibetsu City Hospital, Hokkaido, Japan
[n] Sanraku Hospital, Tokyo, Japan
[o] Yao General Hospital, Osaka, Japan
[p] Infectious Diseases Surveillance Center, National Institute of Infectious Diseases, Tokyo, Japan

ARTICLE INFO

Article history:
Received 17 May 2012
Accepted 30 July 2012

Keywords:
Adverse effects
Blood transfusions
Haemovigilance
Online system
Pilot study

ABSTRACT

Background: A surveillance system for transfusion-related adverse reactions and infectious diseases in Japan was started at a national level in 1993, but current reporting of events in recipients is performed on a voluntary basis. A reporting system which can collect information on all transfusion-related events in recipients is required in Japan.
Methods: We have developed an online reporting system for transfusion-related events and performed a pilot study in 12 hospitals from 2007 to 2010.
Results: The overall incidence of adverse events per transfusion bag was 1.47%. Platelet concentrates gave rise to statistically more adverse events (4.16%) than red blood cells (0.66%) and fresh-frozen plasma (0.93%). In addition, we found that the incidence of adverse events varied between hospitals according to their size and patient characteristics.
Conclusion: This online reporting system is useful for collection and analysis of actual adverse events in recipients of blood transfusions and may contribute to enhancement of the existing surveillance system for recipients in Japan.

* Corresponding author. Address: Department of Safety Research on Blood and Biological Products, National Institute of Infectious Diseases, 4-7-1 Gakuen, Musashimurayama, Tokyo 208-0011, Japan. Tel.: +81 42 848 7120; fax: +81 42 567 2790.
E-mail address: 130hama@nih.go.jp (I. Hamaguchi).

1473-0502/$ - see front matter © 2012 Published by Elsevier Ltd.
http://dx.doi.org/10.1016/j.transci.2012.07.008